



SYNTHESIS AND CHARACTERIZATION OF SILICA NANOCOMPOSITES FOR BONE APPLICATIONS

Pakkath Abdul Rub Sajid, Thiyagarajan Devasena*

Centre for Nanoscience and Technology, Anna University, Chennai, India

Article Received on: 08/03/12 Revised on: 10/05/12 Approved for publication: 20/05/12

*Email: tdevasenabio@sify.com

ABSTRACT

Osteoporosis is a malady leading to bone fracture and results from imbalance in the rate of osteoblastic bone formation with respect to osteoclastic bone degradation.⁶ Nanotechnology raises exciting possibilities for developing novel therapeutic agents for treating osteoporosis.⁶ We use silica-based fluorescent nanoparticles endowed with natural bone-targeting capabilities and express potent pro-osteoblastogenic and anti-osteoclastogenic activation *in vitro* and show the ability to increase bone mineral density *in vivo*. Here, we initially synthesize mesoporous silica nanoparticles by coating with octadecyl trimethoxy silane. The silica nanoparticles thus prepared is chosen as control. Two different samples of silica nanocomposites are prepared; first binding silica nanoparticles with fluorescent dye i.e tetracycline (SiO₂-Tet), the second sample prepared by combining (SiO₂-Tet) with magnetic nanoparticles (cobalt-ferrite solution) to form (SiO₂-Tet-MNP). All these synthesized nanoparticles are characterized using XRD, SEM, FTIR, E-DAX analysis. Post-characterization work plan involves incorporation of silica-based fluorescent nanoparticles into human bones (or in rat bones in case human bones is not at all available). This includes Micro CT-Scanning, Injecting (SiO₂-Tet-MNP) into bone tissues, Quantitating Bone Mineral Density. Finally results are obtained through test outcome which includes estimations of cell mineralization assays, detection of osteoclast formation, nanoparticle association with Bone surface (Incubation with (SiO₂-Tet)/(SiO₂-Tet-MNP) for 2 hours in well-plates), statistical analyses and figures obtained from characterization methods and thereby expressing the property of silica-based fluorescent nanoparticles to increase bone mineral density and combating osteoporosis.

Key words: Osteoporosis, mesoporous silica, octadecyl trimethoxy silane, tetracycline, magnetic nanoparticles, XRD, SEM.

INTRODUCTION

Osteoporosis is a disease of bones that leads to an increased risk of fracture. In osteoporosis the bone mineral density (BMD) is reduced, bone microarchitecture deteriorates, and the amount and variety of proteins in bone is altered. The disease may be classified as primary type 1, primary type 2, or secondary¹. The form of osteoporosis most common in women after menopause is referred to as primary type 1 or **postmenopausal osteoporosis**. Primary type 2 osteoporosis or **senile osteoporosis** occurs after age 75 and is seen in both females and males at a ratio of 2:1. Finally, secondary osteoporosis may arise at any age and affect men and women equally. This form of osteoporosis results from chronic predisposing medical problems or disease, or prolonged use of medications such as glucocorticoids, when the disease is called steroid- or glucocorticoid-induced osteoporosis (SIOP or GIOP).

Osteoporosis is a severe problem leading to bone fracture and occurs due to imbalance in the rate of osteoblastic bone formation with respect to osteoclastic bone degradation. Osteoporosis risks can be reduced with lifestyle changes and sometimes medication; in people with osteoporosis, treatment may involve both. Lifestyle change includes diet and exercise, and preventing falls. Medication includes calcium, vitamin D, bisphosphonates and several others. Fall-prevention advice includes exercise to tone deambulatory muscles, proprioception-improvement exercises; equilibrium therapies may be included. Exercise with its anabolic effect, may at the same time stop or reverse osteoporosis. Osteoporosis is a component of the frailty syndrome.

Nanotechnology is a multidisciplinary field involving the development of engineered devices in the atomic, molecular and macromolecular level, in the nanometre size range.^{2,3} Applications of nanotechnology to medicine and physiology involve the materials and devices to design and interact with the body at subcellular scales with a high degree of specificity, which is potentially translated to targeted cellular

and tissue-specific clinical applications designed to achieve maximum therapeutic efficiency with minimal side-effects³.

Silica-based nanoparticles appear to have good biocompatibility as they are generally thought to be non-toxic *in vivo*. Silica deficiency leads to detrimental effects on the skeleton including skull and peripheral bone deformities, poorly formed joints, defects in cartilage and collagen and disruption of mineral balance in femur and vertebrae⁴. Silicon has also been suggested to play a physiological role in bone formation, although the action of silicon on bone turnover and structure is presently not clear⁵.

Mesoporous silica is a form of silica and a recent development in nanotechnology. The most common types of mesoporous nanoparticles are MCM-41 and SBA-15. Today, mesoporous silica nanoparticles have many applications in medicine, biosensors, and imaging. Mesoporous silica nanoparticles are synthesized by reacting tetraethyl orthosilicate with a template made of micellar rods. The result is a collection of nano-sized spheres or rods that are filled with a regular arrangement of pores. The template can then be removed by washing with a solvent adjusted to the proper pH. In another technique, the mesoporous particle could be synthesized using a simple sol-gel method or a spray drying method. Tetraethyl orthosilicate is also used with an additional polymer monomer (as a template).

The structure of these particles allows them to be filled with a fluorescent dye that would normally be unable to pass through cell walls. The Mesoporous Silica Nanomaterials are then capped off with a molecule that is compatible with the target cells. When they are added to a cell culture, they carry the dye across the cell membrane. These particles are optically transparent, so the dye can be seen through the silica walls. The dye in the particles does not have the same problem with self-quenching that a dye in solution has. The types of molecules that are grafted to the outside of these nanomaterials will control what kinds of biomolecules are allowed inside the particles to interact with the dye.

The present study aims to synthesise and characterise silica nanoparticles as well as the silica nanocomposites for subsequent incorporation into bones in order to reveal the strengthening of bones by silica particles. This will be useful for combating osteoporosis.

Prior to this work, a substantial work on osteoporosis treatment was carried out by using silica nanoparticles⁶. However, the work had a few shortcomings. The previous work made use of certain chemicals like allyl iodide, trimethoxy silane, N-trimethoxysilylpropyl N,N,N-trimethylammonium chloride, methyl (polyethyleneoxy)-propyl trimethoxy silane, N-trimethoxysilylpropyl polyethylene glycol which is very expensive and therefore rare in most laboratories in India and limited lab facilities. So certain modifications were made by replacing rhodamine-B with tetracycline which also plays a major role in bone applications (used as a marker in bone-marrow cancer). N-trimethoxysilylpropyl polyethylene glycol was not available as a reagent but was prepared by mixing equal volumes of trimethoxy propyl silane with poly-ethylene glycol. For preparing magnetic nanoparticle, cobalt chloride was replaced with cobalt acetate and the use of platinum on activated charcoal was omitted.

MATERIALS AND METHODS

Materials

The materials which were used to carry out this experiment were aqueous ammonia, ethanol, distilled water, Tetra-ethoxy silane (TEOS), Octadecyl trimethoxy silane (ODTS), the latter two chemicals being purchased from **Alfa Aesar, a Johnson Matthey company, Massachusetts, U.S.A**. The various chemicals which were used for preparing silica nanocomposites included tetracycline, tri-methoxy propyl silane, ferric chloride trihydrate, cobalt acetate hexahydrate, ferric nitrate nonahydrate, poly-vinyl pyrrolidone solution, poly-ethylene glycol which were all purchased from **Alfa Aesar, a Johnson Matthey company, Massachusetts, U.S.A and Sisco Research Laboratories Private Limited, Mumbai, India**. The equipments used to carry out the entire experiments were magnetic stirrer (at room temperature), centrifuge and high-temperature furnace. The synthesized silica nanoparticles and silica nanocomposites were characterized using various techniques like X-Ray Diffraction, Scanning Electron Microscopy, Fourier Transform Infra-Red Spectroscopy, Atomic Force Microscopy, Energy Dispersive X-Ray Analysis.

Methods

Synthesis of silica nanoparticles by coating with octadecyl trimethoxy silane (ODTS).

3.14 ml of aqueous ammonia was dissolved in 10 ml distilled water and then mixed into 74 ml of absolutely ethanol. To this mixture, added a few ml of tetra ethoxy silane (TEOS). The mixture was subjected to magnetic stirring for 1 hour. After stirring, to this mixture, added another 5 ml of tetra ethoxy silane and 2 ml of octa-decyl trimethoxy silane (ODTS). Silica spheres are obtained after which subjected to stirring again for effective mixing. The mixture was then subjected to centrifugation at 4000 rpm for 10 minutes. After centrifugation, the precipitate was taken in a watch glass and made to dry. The dried precipitate was transferred to a ceramic boat and kept in a high temperature furnace for calcination at 823 K for 6 hrs at air to yield final mesoporous spherical shell silica nanoparticles which was characterized using X-Ray Diffraction, Scanning Electron Microscopy, Energy Dispersive X-Ray Analysis, Fourier Transform Infra-Red.

Synthesis of Nanocomposite 1 SiO₂-Tet.

100 mg of trimethoxy-propyl silane-tetracycline (50 mg of trimethoxy propylsilane + 50 mg of tetracycline) was mixed with 4.3 g of tetraethoxy silane. The whole mixture was dissolved in ethanol. To this, added 1 ml of ammonia and distilled water. The mixture was stirred for 4 hours to facilitate proper mixing and then centrifuged. After centrifugation, fluorescent silica nanoparticle was removed and the supernatant was discarded. The resultant precipitate was dissolved in ethanol. The entire washing process was repeated thrice. The resultant nanocomposite was dispersed in ethanol for surface-modification and finally taken for characterization by Atomic Force Microscopy.

Synthesis of Nanocomposite SiO₂-Tet-MNP.

Initially magnetic nanoparticle solution was prepared using equal masses of cobalt acetate and ferric nitrate and dissolved in distilled water. 40 mg of cobalt-ferrite mixture was dissolved in 1 ml of water and 70 ml of cobalt-ferrite solution was taken. To this solution, added poly vinyl pyrrolidone solution (0.256 g/10 ml of water). The entire mixture was stirred for 24 hours at room temperature. After stirring, the PVP-stabilized cobalt ferrite nanoparticle as separated by adding aqueous acetone and then centrifuged at 4000 rpm for 10 minutes. After centrifugation, the supernatant was discarded and precipitated particles were redispersed in ethanol (10 ml). The process was repeated again and after that, Nanocomposite 1 (SiO₂ -Tet) was added to PVP-stabilized cobalt-ferrite solution. The entire mixture was subjected to polymerization process using aqueous ammonia solution as catalyst (1 ml; 30% wt of ammonia). Now the cobalt-ferrite silica core-shell nanoparticle containing organic dye is formed which was dispersed in ethanol and precipitated out by ultra-centrifugation (18000 rpm, 30 minutes). This washing process was repeated thrice and finally dispersed in ethanol for surface-modification step and taken for characterization using Atomic Force Microscopy.

RESULTS AND DISCUSSION

X-Ray Diffraction (XRD) Analysis

The sample prepared by the precipitation method is characterized using X-ray diffraction for phase confirmation and determination of the grain size.

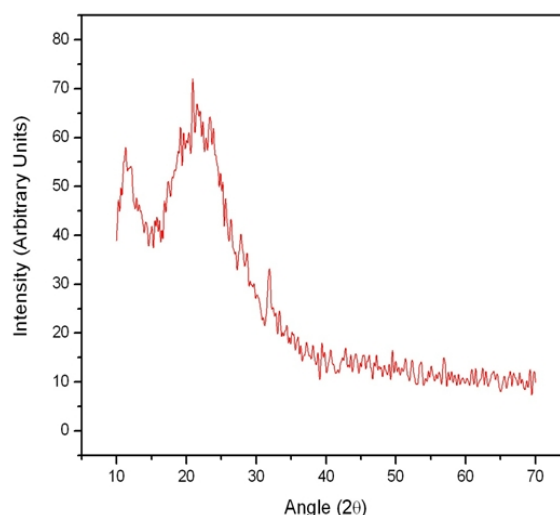


Figure 1 (a) Shows X-ray diffraction pattern of the silica sample.

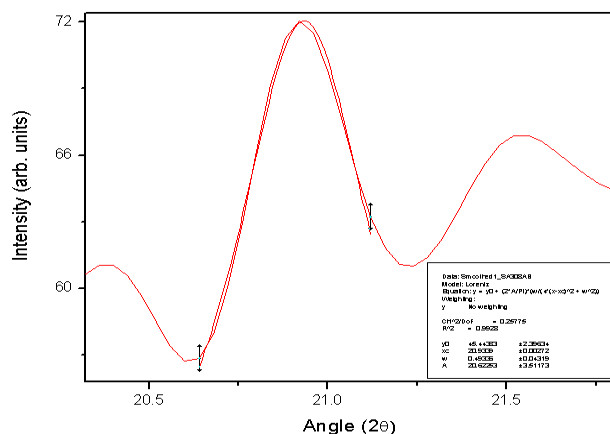


Figure 1.(b) shows the X-ray diffraction pattern of the nanocrystalline mesoporous silica which shows a diffraction peak 2θ at approximately 21° i.e exactly 20.93°.

The information of the particle size is obtained from the full-width at half maximum (FWHM) of the diffraction peaks using the Debye-Scherrer's formula. If the sample is annealed at various temperatures, then particle growth occurs. The average grain size is calculated using the Scherrer's formula given by

$$D = (0.9\lambda) / (\beta \cos \theta),$$

where

D - the average particle diameter,
 λ - the wavelength of Cu K_{α1} line (1.5406 Å),
 β - the full-width half-maximum of the peak at θ
 θ - the diffraction angle of the peak under peak under consideration.

Therefore, $D = 0.9 * 1.54 * 10^{-10} / 0.49336 * \cos(10.467)$
 $= 0.9 * 1.54 * 180 * 10^{-10} / 0.49336 * 0.9833 * 3.14$
 $= 1.386 * 180 * 10^{-10} / 0.4851 * 3.14$
 $= 249.48 * 10^{-10} / 1.5232$
 $= 163.78 * 10^{-10} \text{ m}$
 $= 16.378 \text{ nm}$.

The average particle size of the mesoporous silica was found to be **16.378 nm**.

The weight loss of silica due to calcination from room temperature to 550°C is high due to loss of chemisorbed octadecyl trimethoxyl group and physisorbed water and ethanol.

Scanning Electron Microscopy (SEM) Analysis (mesoporous silica nanoparticles)

SEM images of mesoporous silica synthesised by coating with octadecyl trimethoxy silane was obtained as follows:

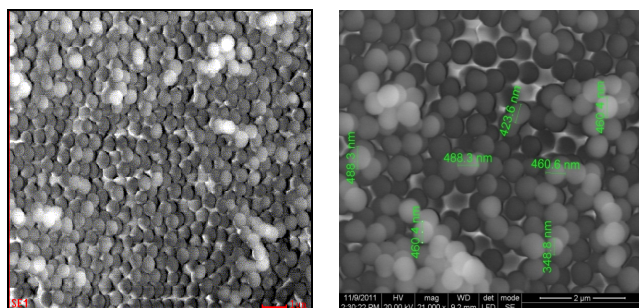


Figure 2(a): Image of mesoporous silica nanoparticles arranged in clusters.

Figure 2(b): High Resolution SEM Image of mesoporous silica nanoparticles at magnification of 21000x, showing particle size above 400 nm. For bone applications, particle size of less than 500 nm are considered as nano-scale.

The morphology and particle size were studied from SEM images of mesoporous silica nanoparticles. The sample synthesized without octadecyltrimethoxy silane shows bimodal particle. The smaller sized particles are present in larger proportion (100 nm, 80%) whereas larger sized particles occur in smaller proportion (300nm, 20%). On adding ODTs, the particle size gets normalized (400 nm, 100%). Octadecyl group in trimethoxy silane molecule increases the electron density around the silane atom. So, the basicity in oxide group is increased. The modified silanol groups show less reactivity and slower reaction with respect to silanol groups from TEOS. As the reaction is slow, the particle size gets increased. Except octadecyl group, other methoxy groups are easily hydrolysable. The alkyl group spreads around the silica sphere and causes steric hinderance for further growth.

Energy Dispersive X-Ray Analysis

E-DX analysis of mesoporous silica nanoparticles was carried out along with SEM result.

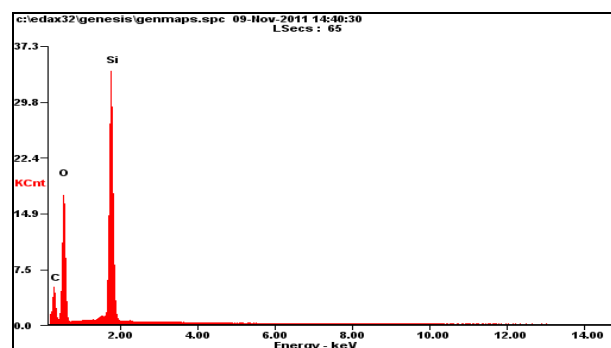


Figure 3 shows E-DAX spectrum of mesoporous silica nanoparticles. E-DAX spectrum of the calcined sample shows a peak for Si,O and C. The small C peak denotes the presence of carbon traces present in carboxyl bonds around silica spheres.

Fourier Transform Infrared Spectroscopy (FTIR) Analysis

FTIR Analysis was carried out for the above product.

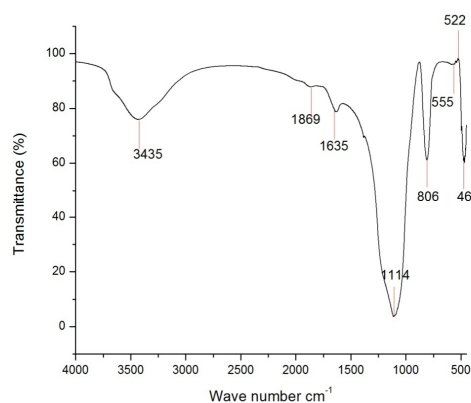


Figure 4 shows FTIR spectrum of mesoporous silica nanoparticles.

The FTIR Spectrum of the synthesized sample shows peaks around 1635 and 3435 cm⁻¹ denoting carboxyl and hydroxyl groups respectively. The adsorption peak belonging to Si-O stretching vibrations of Si-OH bonds appear at 555 and 522 cm⁻¹. The weak peak appearing at 1869 cm⁻¹ belong to the stretching vibrations of C-H bonds and show that a few organic bonds are adsorbed on the spheres. The strong peaks

appearing at 1114, 806, 467 cm^{-1} agree with Si-O-Si bonds, implying the conditions of silicon alkoxide.

Atomic Force Microscopy (AFM) Analysis

AFM analysis was carried out for the nanocomposites 1 (SiO_2 – Tet) and 2 (SiO_2 – Tet-MNP).

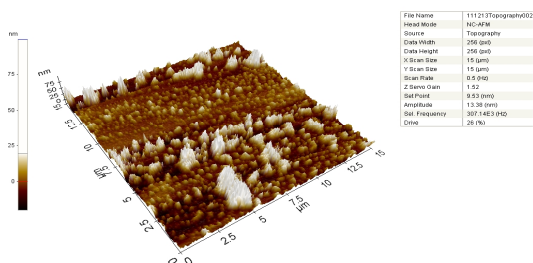


Figure 5(a). AFM Image of nanocomposite SiO_2 – Tet. The size and morphology was studied from AFM images. The size was found to be nearly 50 nm. The nanocomposites were found to be agglomerated in some regions and uniformly dispersed in most regions.

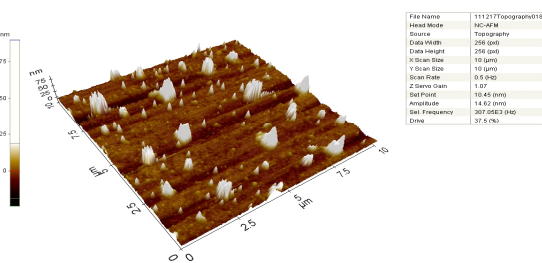


Figure 5 (b). AFM Image of nanocomposite SiO_2 – Tet – MNP. The size and morphology was studied from AFM images. The size was found to be nearly 25 nm. The nanocomposites were found to be agglomerated in some regions and uniformly dispersed in most regions.

Scanning Electron Microscopy (SEM) Analysis (nanocomposite 3)

SEM Analysis was carried out for nanocomposite 3 (SiO_2 – Tet-MNP - PEG)

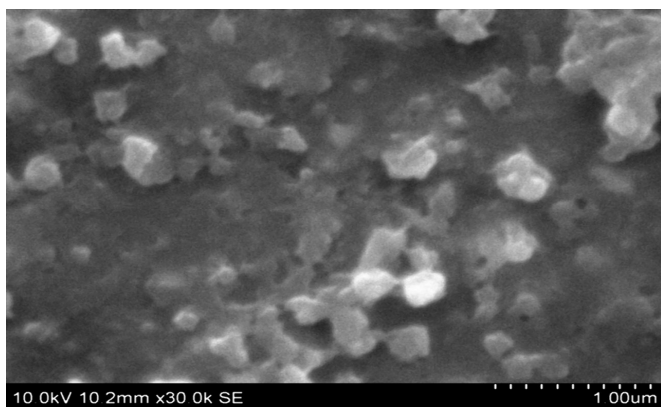


Figure 6 (a). SEM image of nanocomposite 3 (SiO_2 - Tet - MNP – PEG).

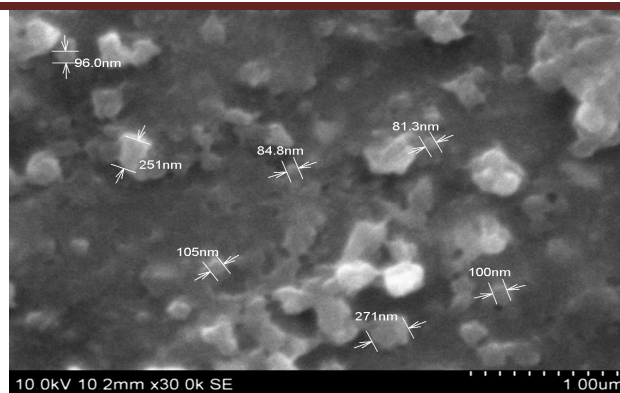


Figure 6 (b). SEM image of nanocomposite 3 (SiO_2 - Tet - MNP – PEG)

The size and morphology of nanocomposite 3 were studied using SEM.

The morphology and particle size were studied from SEM images of silica nanocomposite mixed with tetracycline, magnetic nanoparticle and poly-ethylene glycol. The particle size of the nanocomposite was found to be ranging from 80 nm to 300 nm which is an ideal size for nanocomposites . Some nanocomposites ranging just above 80 nm were found to be spherical in shape whereas those nanocomposites ranging from 100 nm to 300 nm were amorphous or irregular in shape.

SUMMARY & CONCLUSION

Mesoporous silica nanoparticles were synthesized by coating with octadecyl trimethoxy silane.

Silica nanocomposites were synthesized by treatment with tetracycline, magnetic nanoparticles (cobalt-ferrite solution) and mixed with polyethylene glycol.

The work plan involves incorporation of silica-based fluorescent nanoparticles into human bones (or in rat bones in case human bones is not at all available). This includes Micro CT-Scanning, Injecting NP-3 into bone tissues, Quantitating Bone Mineral Density. Finally results are obtained through test outcome which includes estimations of cell mineralization assays, detection of osteoclast formation, nanoparticle association with Bone surface (Incubation with NP 1/NP 2 for 2 hours in well-plates), statistical analyses and figures obtained from characterization methods and thereby expressing the property of silica-based fluorescent nanoparticles to increase bone mineral density and combating osteoporosis.

The silica nanocomposite obtained from our study can be considered as an ideal candidate for bone applications. Hence, the incorporation of the nanocomposite into bones for strengthening the deformed bones and for combating osteoporosis is underway in our laboratory. The procedure involves Micro CT-Scanning, Injecting NP-3 into bone tissues, Quantitating Bone Mineral Density, estimations of cell mineralization assays, detection of osteoclast formation, study of nanoparticle association with Bone surface (Incubation with NP 1/NP 2 for 2 hours in well-plates).

REFERENCES

1. Brian K Alldredge; Koda-Kimble, Mary Anne; Young, Lloyd Y.; Wayne A Kradjan; B. Joseph Guglielmo (2009)., *Applied therapeutics: the clinical use of drugs*. Philadelphia: Wolters Kluwer Health/Lippincott Williams & Wilkins. pp. 101–3. ISBN 0-7817-6555-2.
2. Navalkhe & Nandedkar (2007)., *Ind J. Exp Biol.* 45:160-165.
3. Sahoo et al (2007)., *Nanomedicine* 3: 20-31.
4. Martin (2007)., *J. Nutr. Health Aging* 11: 94-97.
5. Seaborn & Nielsen(2002)., *Biol.Trace Element Research* 89: 239-250.
6. Mervyn Neale Weitzmann, George Richard Beck, Jin-Kyu Lee; *Silica based nanomaterials and methods of stimulating bone formation and suppressing bone resorption through modulation of NF-KB*, 2007.
7. Agger J R, Anderson M W, Pemble M E, Tarasaki O, Nozue Y (1998), *J Phys. Chem B*,102,3345.
8. Bogush and Zukoski (1998), *Journal of Non-crystalline solids* 104, 95.
9. Boyce et al., *Bone* 25:137-139(1999); Fransozo et al. (1997)., *Genes Development* 11:3482-3496 .
10. Iler R K(1979).; *The Chemistry of Silica*, Wiley, New York.
11. Kim K D, Kim H T (2002); *J. Sol-Gel Science & Technology*; 25, 183.
12. Li Y, Xu C, Wei B, Zhang X, Zheng M, Wu D, Ajayan P M (2002);*Chem Mater* 14, 183.
13. Masuda R, Takahashi W, Ishii M (1990); *Journal of Non-crystalline solids* 121, 389.
14. McClung et al. (2006)., *N Engl J Med* 354: 821-823
15. Park S K, Kim K D, Kim H T (2002); *Coll surf A, Physicochem. Eng Asp.*197 ;7.
16. Sacks M D & Tseng T Y (1984), *Journal of American Ceramic Society*, 67 526.
17. Sadasivan S, Rasmussen D H, Chen F P, Kannabiran R K (1998); *Coll surf A, Physicochem. Eng Asp.* 132; 45.
18. Shan Y, Gao L, Zheng S (2004); *Mater Chem Phys* 88,192.
19. Stober W, Fink A, Bohn E (1968); *J Coll Interf Science*, 26; 62.
20. Taira M, Yamaki M (1995); *Journal of Material Science and Material Medicine*, 6; 197.
21. Teitelbaum (2000); *Science* 289: 1504-1508.
22. Yamashita D, Mori M H, Maekawa T (1992) , *Journal of Ceramic Society, Japan* 100; 1444.

Source of support: Nil, Conflict of interest: None Declared